Calculated shallow-donor-level binding energies in GaAs-$Al_xGa_{1-x}As$ quantum wells

M. Stopa and S. DasSarma
Department of Physics, University of Maryland, College Park, Maryland 20742-4111
(Received 24 October 1988; revised manuscript received 1 May 1989)

We numerically solve Schrödinger's equation for a single electron located in a GaAs-$Al_xGa_{1-x}As$ quantum well with a shallow Coulombic donor impurity either in the well or in the barrier, as a function of well width, well depth, and impurity position. We calculate the binding energy of the ground state and of the first two "*s*-like" excited states and also the binding energy of the lowest "*p*-like" excited state. We compare our exact numerical results for the ground-state binding energy with earlier variational calculations and show that they are nearly coincident with these calculations. We calculate the electronic charge density as a function of impurity position and show that the asymmetry in the charge density peaks and then decreases as the impurity is taken from the center of the well to the edge and then into the barrier.

I. INTRODUCTION

It is well known that when a shallow donor impurity is placed in a bulk semiconductor, a bound electronic state may form below the conduction band. This bound state can be described as a superposition of the states in the bottom of the band.[1] When an electron is placed in a quantum well, however, the band structure is broken into a set of discrete subbands by the confinement in the z direction (perpendicular to the well interfaces). In this case the character of the resulting impurity bound state changes. The potential no longer possesses, even approximately, spherical symmetry. In addition, the binding energy, which is now defined as the energy one must supply in order to free the electron for effective-mass-like motion in the plane parallel to the well (that is, to place it in the lowest subband of the well) is found to increase from the bulk binding energy. The binding energy continues to increase as the well is made narrower but peaks and turns over for very narrow wells ($\simeq 50$ Å).

Photoluminescence studies[2] and electronic Raman scattering[3] have recently been used to determine the energy levels of shallow (silicon) dopants in GaAs-$Al_xGa_{1-x}As$ multiple-quantum-well structures. These results have shown good agreement with variational calculations[4–7] of the energy levels of shallow donors with hydrogeniclike trial wave functions. Experiment and calculation have both examined the variation of binding energy with well width, well depth, and impurity position.

In this paper we present an exact numerical solution of Schrödinger's equation for a single electron and a single shallow Coulombic impurity in a GaAs-$Al_xGa_{1-x}As$ quantum well. This solution follows Vinter's treatment[8] of the impurity in a silicon metal-oxide-semiconductor (MOS) structure. We compute both the energy spectrum and the associated eigenfunctions as a function of well width, well depth, and impurity position. We find that our binding energies of the ground state are nearly coincident with those of the variational calculations. We also show that the charge distribution varies markedly with impurity position and that for an impurity located far (approximately two well widths) into the barrier the charge distribution is very nearly symmetric about the well center. One significant result of our exact numerical calculation is that it substantiates the accuracy of the simpler variational calculations for obtaining shallow-donor ground-state energies in quantum wells.

II. DESCRIPTION OF THE CALCULATION

In cylindrical coordinates with the z axis through the impurity and normal to the well interface, our Hamiltonian is

$$H=\frac{-\hbar^2}{2m^*}\nabla^2+V_0\Theta(|z|-a/2)-\frac{Ze^2}{\kappa[R^2+(z-z_0)^2]^{1/2}}\ , \tag{1}$$

where V_0 is the well depth (which is related to the aluminum concentration in the barrier), a is the well width, Z is the impurity charge which we will henceforth take to be $+1$, z_0 is the distance of the impurity from the center of the well, κ is the lattice dielectric constant, and m^* is the effective mass. We have thus made the standard effective-mass approximation for the band structure, which is known to be valid for GaAs. We use scaled atomic units wherein $\hbar=e^2/2\kappa=1$, the unit of length is the Bohr radius $a^*=\kappa/m^*e^2=98.7$ Å, and the unit of energy is the effective Rydberg $\mathcal{R}^*=m^*e^4/2\kappa^2=5.8$ meV.

We write $H=H_0+H_1$ where

$$\begin{aligned} H_0(z)&=-\frac{\partial^2}{\partial z^2}+V_0\Theta(|z|-a/2)\ , \\ H_1(z)&=-\frac{\partial^2}{\partial R^2}-\frac{1}{R}\frac{\partial}{\partial R}-\frac{1}{R^2}\frac{\partial^2}{\partial\Theta^2} \\ &\quad -\frac{2}{[R^2+(z-z_0)^2]^{1/2}}\ . \end{aligned} \tag{2}$$

Solving the one-dimensional Schrödinger equation for H_0 we get the usual complete set of subband wave functions $H_0\xi_n = E_n\xi_n$. We use this set to expand the total wave function:

$$\Psi(R,\phi,z) = e^{im\phi}\sum_n \xi_n(z) f_n(R) , \tag{3}$$

where the azimuthal symmetry of the problem gives the simple ϕ dependence with m, the azimuthal quantum number, an integer. We expand the radial functions above in Bessel functions and integrate the resulting differential equation from the origin to a midpoint R_0 and from a suitably chosen "infinity" in to R_0. The matching of the wave function at that point provides a set of linear equations which depends upon the energy and the boundary values of the components of the wave function at zero and infinity. A determinantal condition on the energy is then obtained and the integration procedure is iterated until a zero of the determinant is found. The details of this procedure are well presented in Vinter's paper and we will not repeat them here.

III. APPROXIMATIONS AND SOURCES OF INACCURACY

Within the confines of the model we can achieve essentially arbitrary accuracy given sufficient computation time. The physical assumptions of the model are (i) the effective-mass approximation (as already noted); (ii) an assumption that the dielectric mismatch between GaAs-$Al_xGa_{1-x}As$ is negligible. We expect this to affect the energies by considerably less than 1%; (iii) single electron, single impurity, single well with no overlap between adjacent wells. The accuracy of our computation is limited by two factors. First, we can obviously only expand the solution in a finite number of subbands. We can vary the number of subbands, though, to check the accuracy of any given choice. Second, we must cut off the integration procedure at some finite R_{max}. This cutoff effectively sets the impurity potential to zero outside R_{max}. Again we can vary R_{max} to test the sensitivity of the results to the cutoff. Generally, the deep-lying states are insensitive to a choice of cutoff, but the states near the lowest subband are more significantly affected. Thus, the percentage error for weakly bound states can be appreciable. For both the subband and integration cutoff the effect will always be to underestimate the binding energies. Hence, our quoted binding energies are lower bounds.

IV. RESULTS

To facilitate comparison with experiment we present, in addition to several plots described below, a table of selected results (Table I). The principal division in the

TABLE I. Impurity binding energies. (a) shows binding energies for an impurity centered in the well with a varying well width and two well depths, $25\mathcal{R}^*$ and $50\mathcal{R}^*$. (b) shows binding energies with varying impurity position, a fixed well depth of $55.67\mathcal{R}^*$, and three well widths, 100, 250, and 400 Å. The number in parentheses following a datum represents the numerical uncertainty in the final one or two digits of that datum, as described in the text. The uncertainties in the excited states have not been estimated. All energies are in $\mathcal{R}^*$.

(a) Binding energies vs well width

	State	25 Å	50 Å	100 Å	150 Å	200 Å	300 Å	400 Å	600 Å	800 Å
$V_0=25\mathcal{R}^*$	1s	2.180(0)	2.270(0)	2.057(0)	1.845(0)	1.810(0)	1.543(11)	1.403(0)	1.218(0)	1.113(54)
	2s	0.358	0.364	0.351	0.338	0.327	0.310	0.297	0.278	0.265
	3s	0.0846	0.142	0.139	0.0742	0.0679	0.0527	0.0499	0.0459	0.0435
	1p	0.430	0.433	0.429	0.421	0.413	0.396	0.376	0.353	0.331
$V_0=50\mathcal{R}^*$	1s	2.524(0)	2.457(0)	2.145(0)	2.081(0)	1.823(0)	1.574(12)	1.415(0)	1.234(0)	1.130(43)
	2s	0.378	0.375	0.357	0.342	0.330	0.312	0.298	0.280	0.274
	3s	0.0947	0.0931	0.0844	0.0764	0.0695	0.0530	0.0502	0.0459	0.0462
	1p	0.438	0.438	0.432	0.423	0.414	0.397	0.381	0.354	0.331

(b) Binding energies vs impurity position

	State	$z_0=0$	$z_0=\frac{1}{8}$	$z_0=\frac{1}{4}$	$z_0=\frac{3}{8}$	$z_0=\frac{1}{2}$	$z_0=\frac{3}{4}$	$z_0=1$	$z_0=2$
$a=100$ Å	1s	2.156(0)	2.103(20)	1.939(41)	1.697(38)	1.464(20)	1.157(4)	1.011(20)	0.7723(5)
	2s	0.356	0.352	0.339	0.319	0.297	0.263	0.238	0.174
	3s	0.0937	0.0840	0.0818	0.0748	0.0633	0.116	0.109	0.090
	1p	0.432	0.429	0.422	0.411	0.398	0.372	0.347	0.271
$a=250$ Å	1s	1.688(0)	1.616(21)	1.408(4)	1.113(14)	0.854(6)	0.608(4)	0.500(3)	0.497(1)
	2s	0.319	0.315	0.298	0.263	0.235	0.198	0.175	0.121
	3s	0.131	0.130	0.125	0.118	0.106	0.093	0.084	0.056
	1p	0.407	0.399	0.379	0.352	0.326	0.282	0.248	0.170
$a=400$ Å	1s	1.417(0)	1.364(8)	1.203(4)	0.896(9)	0.634(1)	0.430(1)	0.346(0)	0.244(0)
	2s	0.298	0.298	0.284	0.245	0.202	0.164	0.142	0.095
	3s	0.125	0.126	0.122	0.111	0.095	0.079	0.067	0.033
	1p	0.382	0.372	0.344	0.309	0.277	0.228	0.195	0.116

table is between binding energies versus well width, with well depth fixed and the impurity centered in the well on the one hand [Table I(a)], and binding energies versus impurity position, with well depth and well width fixed, on the other hand [Table I(b)].

We also quote numerical uncertainties in Table I. The number(s) in parentheses following the datum represent(s) the uncertainty in the final digit(s) of that datum. Thus 1.318(43) is equivalent to 1.318 ± 0.043. As described in Sec. III, expanding the solution in a finite (as opposed to infinite) number of subbands and cutting off the integration at a finite $R_{\max}$ cause the principal uncertainty in the numerical results. The quoted uncertainties represent the difference between the given datum and the same datum recalculated with one subband fewer or with $R_{\max}$ decreased by 25%, whichever difference is larger. We have only quoted uncertainties for the ground-state binding energy. Since the excited states are close to the free-particle continuum it is difficult to determine the accuracy of the absolute size of the binding energy. Thus we present these data with the caveat that only the trends with impurity position or well width should be taken seriously and that the absolute value of the binding energy should be viewed with some caution.

Note that, in contrast to the excited states, the uncertainty in the ground-state binding energy is never more than 3% and is often substantially less.

We note that the azimuthal quantum number (m) for an impurity in a well is not equivalent to the angular-momentum quantum number (l) for a hydrogen atom. Indeed, it is the quantum number for the z component of angular momentum, just as m usually is in hydrogen notation. The hydrogenic angular functions characterized by l are Legendre polynomials (or spherical harmonics). For the impurity in a well the angular functions characterized by m are simply $\exp(im\phi)$'s. Nonetheless, many authors in the literature use hydrogenic notation, $1s$, $2s$, $2p$, etc., to denote the bound states of impurities in quantum wells. Note, however, that if the letter ($s,p,d,f,\ldots$) is to signify the m quantum number, there is no prohibition in this case against a $1p$ state (or $1d$, or $1f$, etc.). Therefore, it is actually misleading to omit $1p$ in analogy with the hydrogen atom. Physically this arises because angular momentum is not conserved when a hydrogenic atom is subjected to a z-dependent potential. The z component of angular momentum, however, remains a good quantum number. The physics is made more clear when we present a simple perturbative calculation of a hydrogenic impurity in a *very* wide quantum well. In the limit of infinite well width the states are just the hydrogenic impurity states. As the well walls move in from infinity, states of different n and l are mixed by the wall perturbation. Mixture does not occur between states of different m. Symmetry under inversion demands the existence of one more quantum number, the parity. This is evidenced by the fact that the perturbation does not mix *all* states of differing l, but only mixes states for which Δl is even. (Contrast this with the Stark effect where, since the perturbation is odd in z, only Δl odd mixing occurs.)

Figure 1 presents the results of such a perturbation calculation where we have subjected the $m=0$, $n=1$, 2, and 3 states of a hydrogenic impurity to a wall perturbation. The principal result is that, for a well depth of $25\mathcal{R}^*$, the splitting of the $n=3$ level becomes comparable to the spacing between the $n=2$ and $n=3$ levels for a well width of about 5500 Å. The $n=2$ level splits a comparable amount for a well width around 2000 Å.

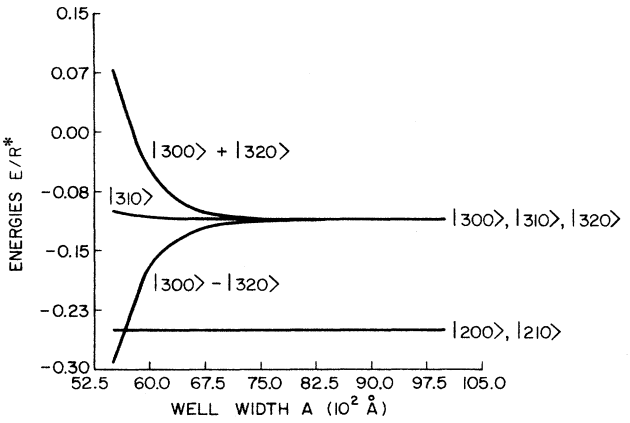

FIG. 1. Three-dimensional hydrogenic energy levels subject to the perturbation of a wide quantum well, as a function of well width. The well depth is $25\mathcal{R}^*$. The levels shown all have $m=0$. At the right (wide well limit) $3s$, $3p^0$, and $3d^0$ are degenerate as are $2s$ and $2p^0$. At the left the $n=2$ levels are still degenerate but the $n=3$ levels have been split as shown. The ket notation in the figure is the standard n,l,m hydrogen-state notation.

In our notation, the leading number designates the principal quantum number, the energy, and the letter designates the m quantum number, which corresponds to the angular exponential and to the order of the Bessel

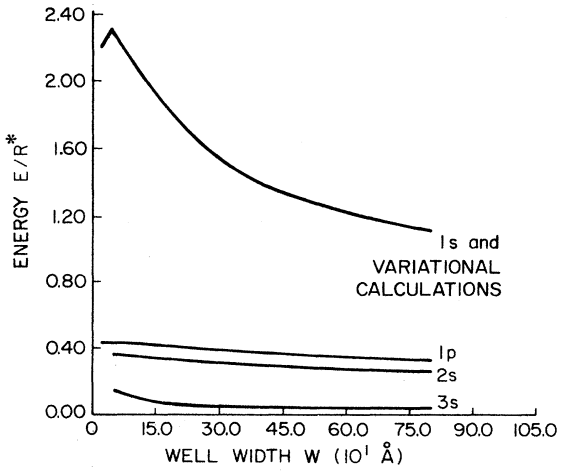

FIG. 2. Impurity binding energies as a function of well width. The top curve represents both our ground-state binding energies and those of the variational calculations (Ref. 4); the remaining curves, from top to bottom, are from our calculations for the binding energies of the $1p$, $2s$, and $3s$ states, respectively.

function in the radial wave function. The point of our analysis here is that these states cannot be identified as specific linear combinations of hydrogenic states, with the exception of the $1s$ state, which remains unchanged down to fairly small well sizes. The only thing one can say is that a state of given m is a mixture of hydrogenic states of the same m, and that parity is conserved. Hence, the use of hydrogenic notation to denote impurities in quantum wells is not only misleading it is wrong.

In Fig. 2 we plot the impurity-centered binding energy of the ground state and first three excited states ($1p, 2s, 3s$) as a function of well width. Note that the $1p$ state is uniformly more tightly bound than the $2s$ state, and so represents the first excited state. The well depth is $25\mathcal{R}^*$. Assuming that the conduction-band discontinuity is 55% of the band gap, this corresponds to an aluminum concentration of $x=0.12$ in the barrier. Upon plotting the variational calculations of Greene and Bajaj[7] for the same well depth we discover that the results are coincident to within the limits of numerical accuracy. Thus, the top curve represents both our results and those of the variational calculations, as marked.

Figure 3 illustrates the variation of binding energies with impurity position in the well for various well widths. (Our choice of the rather odd well depth of $55.67\mathcal{R}^*$ was made to facilitate comparison with some of the variational results presented in Ref. 7.) The binding energy of the ground state [Fig. 3(a)] falls off quite rapidly from its well-centered maximum. The curves then flatten out as the impurity is moved into the barrier. The binding energy remains finite for as large a distance between impurity and well center as we computed (two well widths). In

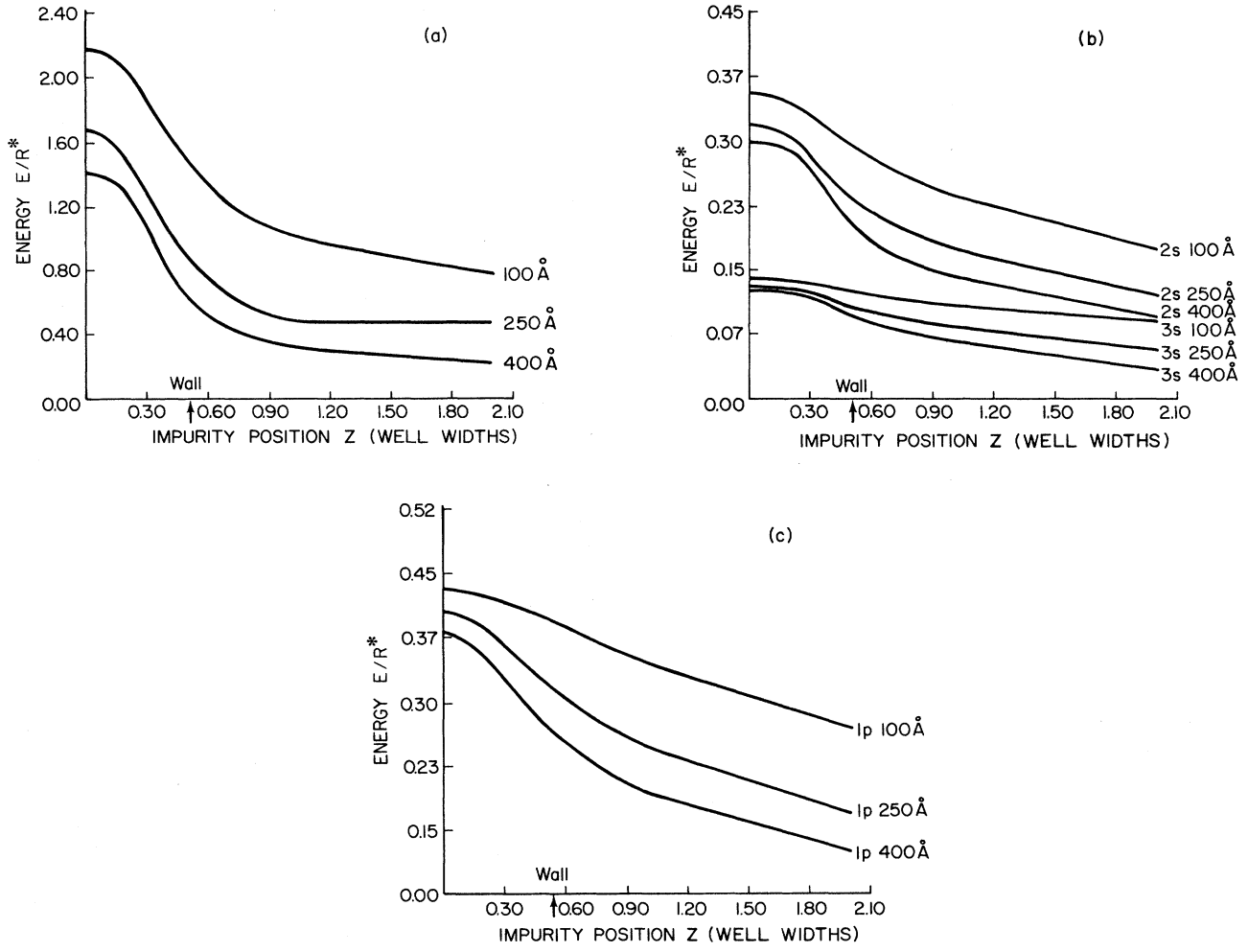

FIG. 3. Impurity binding energies as a function of impurity position, for various well widths. (a) shows the variation of the ground-state binding energy with impurity position for (from top to bottom) 100, 250, and 400 Å. (b) shows the binding energies of the $2s$ and $3s$ states. The top three curves are the $2s$ energies for (from top to bottom) 100, 250, and 400 Å. The bottom three curves are the $3s$ energies for the same well widths in the same order. (c) shows the variation of the $1p$ energies for the same three well widths which again occur in the same order. The edge of the well is indicated by an arrow in each plot. Note that the electron remains bound when the impurity is inside the barrier for as far in as we chose to put it.

Fig. 2(b) we see again that the fractional change in the excited-state binding energies with changing impurity position is less than that of the ground-state binding energies; just as in the case of varying well *width* (Fig. 2).

In Fig. 3(c) we plot the binding energies of the $1p$ states, for various well widths, as a function of impurity position. These curves are quite similar in form to the excited s states and once again they are uniformly more tightly bound than the $2s$ state (for the same well width and impurity position).

One conclusion we can draw from the variation of impurity binding energy with impurity position concerns the case of quantum wells doped sparsely but homogeneously through a range of z_0 values with hydrogenic im-

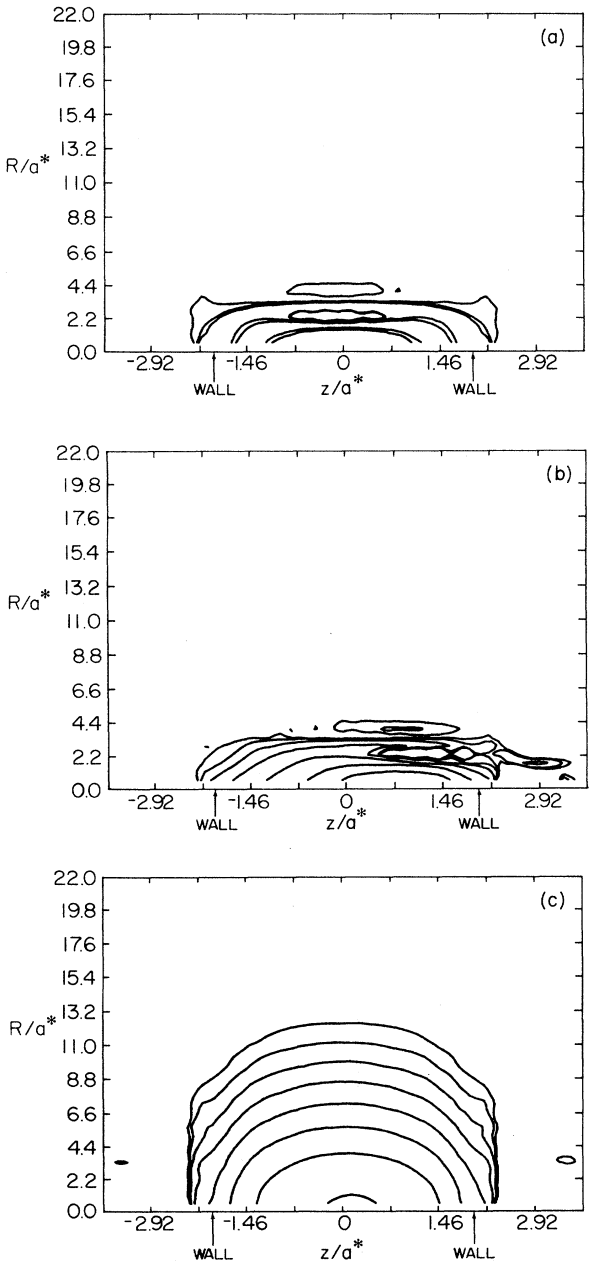

FIG. 4. Contour plot of the electron charge density bound to the impurity in the lowest state with the impurity: (a) at the center of the well, (b) halfway from the well center to the well wall, and (c) one full well width from the center of the well. Contours are logarithmic with two contours per decade. Well width is 400 Å, depth is $55.67\mathcal{R}^*$.

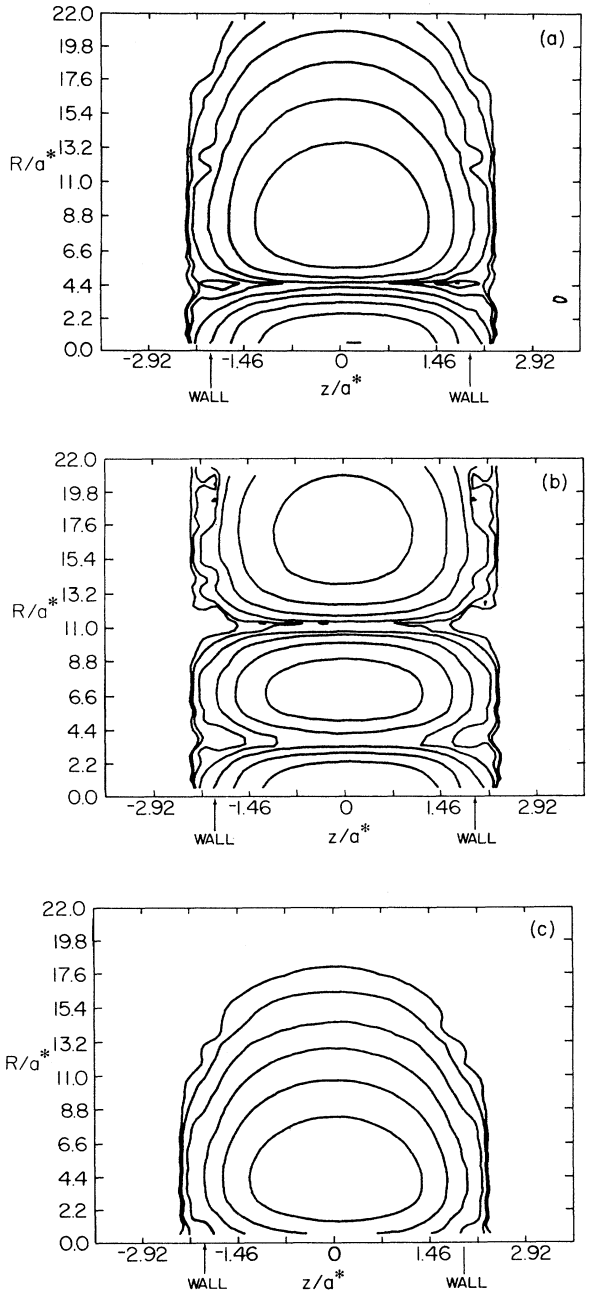

FIG. 5. Contour plots of the various typical excited states. (a) shows a $2s$ state, (b) shows a $3s$ state, and (c) shows a $1p$ state. For all three the well width is 400 Å, the depth is $55.67\mathcal{R}^*$, and the impurity is located in the barrier, 400 Å from the center of the well.

purities. Such doping trivially creates an effective band of energies whose energy width is simply given by the difference between the binding energies of an impurity at the center of the well (or wherever doping begins) and one at the outer edge of the homogeneously doped region. To be concrete, if we dope a 400-Å well homogeneously with silicon impurities (such as we are considering here) from the center of the well out to 800 Å from the center of the well (600 Å into the barrier), then the range of impurity positions spanned by the abscissa in Fig. 3(a) is occupied by impurities. (The density with which the impurities cover this range depends, of course, on the total number of dopants which we use.) Thus, all the corresponding energies (on the 400-Å curve) are available single-electron energies. The bandwidth in this case is given approximately by $1.35\mathcal{R}^*$ (well-centered impurity) minus $0.25\mathcal{R}^*$ (outer-edge energy), or $1.1\mathcal{R}^* \approx 6.4$ meV, which can be taken as an effective impurity bandwidth arising from homogeneous doping.

The variation of the probability densities $|\Psi_m(R,\phi,z)|^2$ with increasing impurity distance from the well center (and, hence, decreasing binding energy) is shown in Fig. 4. When the impurity is centered in the well [Fig. 4(a)] the probability density is naturally symmetric about the well center. When the impurity is halfway from the center of the well to the well wall [Fig. 4(b)], the probability density is similarly displaced, although the wave function suffers some odd collisional effects with the wall. The radial confinement also decreases in this case due to the decreased binding energy. In Fig. 4(c) the impurity is one full well width from the center of the well (i.e., one-half of a well width into the barrier). Here we notice that the electron has resumed its symmetry with respect to the well center, while extending still further in the radial direction. The symmetry of the electronic density distribution for an impurity outside the well to one side is easily explained. The overall strength of the shallow impurity is small compared with the depth of the well. Typical shallow impurities in bulk semiconductors have binding energies of a few meV to a few tens of meV. Well depths (conduction-band discontinuities), on the other hand, are of the order of hundreds of meV. Since the height of the well barrier is large compared with the depth of the impurity potential, the shape of the electronic density distribution is determined largely by the effective potential *within the well.* In particular, the *gradient* of the effective potential in the well decreases as the impurity moves away from the well. Consequently, the asymmetry of the density distribution decreases since the "floor" of the well is becoming less tilted.

In Figs. 5(a), 5(b), and 5(c), we present contour plots for typical excited states: $2s$, $3s$, and $1p$, respectively. The radial distribution of the s states acquires an additional lobe for each higher principal quantum level. The $1p$ state has a single density maximum. This maximum is displaced from the symmetry axis and, in three dimensions, the surfaces of constant density are toroidal.

Finally, in Fig. 6 we present contour plots for *scattering* solutions to Schrödinger's equation. Figure 6(a) is a contour plot for an electron *when no impurity is present.* Thus the solution displayed is just a plane wave associated with the lowest subband expression in cylindrical coordinates. We present this for comparison with Fig. 6(b), which is a scattering solution with impurity present. The electronic energy here is $1\mathcal{R}^*$, which places it between the first and second subbands. For any energy above the lowest subband the electron can undergo free effective-mass-like transport in the plane parallel to the well interface. Thus asymptotically, the given solution is simply a phase-shifted cylindrical-coordinate equivalent of a plane-wave solution. The phase shift of the wave function inward toward the attractive scatterer can be seen by comparing Figs. 6(a) and 6(b).

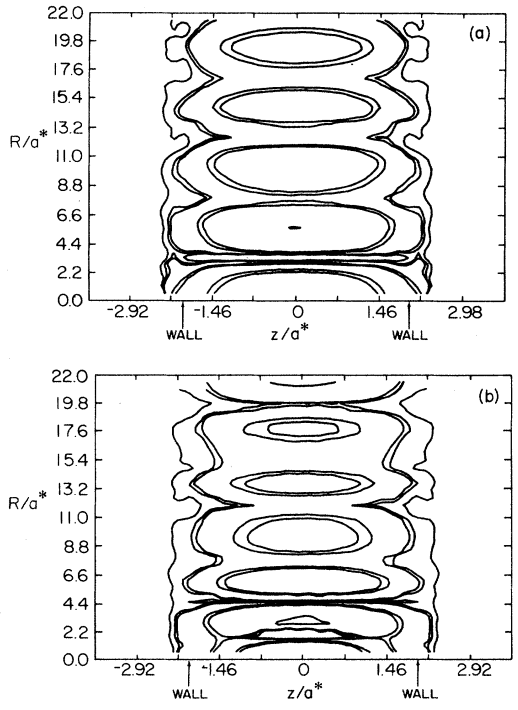

FIG. 6. Contour plots of scattering solutions to Schrödinger's equation. The well width is 400 Å and the well depth is $55.67\mathcal{R}^*$. (a) shows a free plane wave in the absence of the impurity. (b) shows a scattering solution when the impurity is at the center of the well. The electronic energy is $1\mathcal{R}^*$.

V. CONCLUSION

We have solved Schrödinger's equation for the Coulombic electron bound to and scattering from a single impurity embedded in or adjacent to an $Al_xGa_{1-x}As$-GaAs quantum well. We have found that the energy spectrum of the lowest state agrees well with earlier variational calculations of the spectrum. This agreement exists for both the magnitude of the binding energies as well as for the trends of those energies with well width and impurity position. We have presented contour plots of the electron densities both for bound states and for scattering states. We have seen that the electron remains bound to the impurity, albeit more extended in the radial direction, even when the impurity is placed in the barrier

of the well. Further, we have shown that the electronic density reaches a maximum asymmetry as the impurity is moved from the center of the well toward the edge, and returns to a symmetric shape as the impurity moves further into the barrier. This effect is seen to result from the large size of the well depth in comparison to the overall strength of the impurity. Finally, we have presented contour plots of characteristic excited states and scattering states. For excited states we have seen an additional node of the wave function for each increasing level of excitation. For scattering states we have seen the harmonic variation of the radial wave function and we have noticed the inward phase shift of the wave function in comparison with the plane-wave solution in cylindrical coordinates in the absence of any impurity.

ACKNOWLEDGMENTS

We would like to thank the U.S. Army Research Office and the U.S. Office of Naval Research for their support in this research. The work has been supported by the U.S. Department of Defense. We would like to thank the University of Maryland Computing Center for computing time and consulting assistance. We are most pleased to thank Dr. Phillip Sterne for many valuable conversations and expert assistance throughout this work. The work is also supported by the Joint Program for Advanced Electronic Materials sponsored by the U.S. Department of Defense through the Laboratory for Physical Sciences, University of Maryland.

[1]W. Kohn, in *Solid State Physics, Advances in Research and Applications,* edited by F. Seitz and D. Turnbull (Academic, New York, 1958), Vol. 5, p. 257.

[2]B. V. Shanabrook and J. Comas, in Proceedings of the Fifth International Conference on the Electronic Properties of 2D Systems, Oxford, England, 1983 [Surf. Sci. **142**, 504 (1984)].

[3]B. V. Shanabrook, J. Comas, T. A. Perry, and R. Merlin, Phys. Rev. B **29**, 7096 (1984).

[4]G. Bastard, Phys. Rev. B **24**, 4714 (1981).

[5]C. Mailhiot, Y. C. Chang, and T. C. McGill, Phys. Rev. B **26**, 4449 (1982).

[6]R. L. Greene and K. K. Bajaj, Solid State Commun. **45**, 825 (1983).

[7]For a review of variational calculations, see R. L. Greene and K. K. Bajaj, Solid State Commun. **53**, 1103 (1985).

[8]B. Vinter, Phys. Rev. B **26**, 6808 (1982).

[9]S. Chauduri, Phys. Rev. B **28**, 4480 (1983).